Proceedings of the 17th World Congress
The International Federation of Automatic Control
Seoul, Korea, July 6-11, 2008

Distributed Formation Control for Target-enclosing Operations based on a Cyclic Pursuit Strategy

Shinji Hara * **Tae-Hyoung Kim** ** **Yutaka Hori** ***

* *Department of Information Physics and Computing, The University of Tokyo, Tokyo 113-8656, JAPAN (e-mail: Shinji_Hara@ipc.i.u-tokyo.ac.jp)*
** *CREST, Japan Science and Technology Agency, 4-1-8 Honcho, Kawaguchi-shi, Saitama 332-0012, Japan (e-mail: Kim_Tae_Hyoung@ipc.i.u-tokyo.ac.jp)*
*** *Department of Mathematical Engineering and Information Physics, The University of Tokyo, Tokyo 113-8656, JAPAN (e-mail: t60539@mail.ecc.u-tokyo.ac.jp)*

Abstract: This paper studies a design methodology of a distributed cooperative controller for target-enclosing operations by multiple dynamic agents. To this end, we first present an on-line path generator design method based on a cyclic pursuit scheme. Then, we provide the stability condition which the developed path generator should satisfy. This condition is derived based on a simple stability analysis method for large-scale linear systems with generalized frequency variable. The formation control scheme combined with a cyclic pursuit based distributed on-line path generator satisfying the derived stability condition guarantees the required global convergence property with theoretical rigor. Simulation examples illustrate its distinctive features and the achievement of a desired pursuit pattern.

1. INTRODUCTION

Formation control which coordinates the motion of relatively simple and inexpensive multiple agents is one of the essential technologies that enable agents to cover a larger operational area and achieve complex tasks [Marshall et al., 2004, Olfati-Saber et al., 2007]. Recently, Kim and Sugie [2007] proposed a distributed on-line path planning scheme based on a modified cyclic pursuit strategy for target-enclosing operations by multi-agent systems. Despite its simple but particularly effective nature for target enclosing tasks, it could be a considerable drawback in real implementations that each agent is assumed to be a point mass with full actuation. That is, since agent's dynamics is not explicitly considered in path planning, their approach may suffer from the potential problem that each agent cannot track its designed trajectory precisely. In this case, the global convergence of multiple agents to the designated formation may not be achieved. It is therefore required for the improvement of its real implementability to develop a simple distributed on-line path planning strategy for multiple agents which generates the feasible trajectories under the explicit consideration of agent's dynamics and guarantees the global convergence property.

Regarding formation control with dynamic agents, Hara et al. [2007a] proposed a novel technique to analyze the characteristics of large-scale linear systems. To this end, they first introduced the notion of a linear system with a generalized frequency variable; this system denoted as $\mathcal{G}(s)$ is developed by just replacing transfer function's 's' variable in the original system $L(s)$ with a rational function '$\phi(s)$', i.e., $\mathcal{G}(s) := L(\phi(s))$. One of the examples of the systems which may retain generalized frequency variables is a class of formation control for multi-agent systems. Then, they developed a simple unified framework to analyze controllability, observability and stability of the hierarchical system $\mathcal{G}(s)$. Specifically, they presented the stability condition of $\mathcal{G}(s)$ in relation to the pole locations of $L(s)$ in the complex plane and the regions which $\phi(s)$ maps the right-half complex plane to. These results probably make a big contribution to the development of a cyclic pursuit based distributed on-line path planning scheme which guarantees the global convergence property with theoretical rigor.

This paper proposes a distributed cooperative control based on a cyclic pursuit strategy for target-enclosing operations by multiple agents. Here, it is assumed that n agents, which have common system dynamics and identical local controllers, are randomly dispersed in 3D space. The system of each agent combined with a controller is denoted by $H(s)$. In this paper, we first present an on-line path generator design method based on a cyclic pursuit scheme, which was proposed by Kim and Sugie [2007]. Then, based on the results of Hara et al. [2007a], we derive a stability condition which the above cyclic pursuit based on-line path generator should satisfy to guarantee the formation stability. This is described in relation to the pole locations of the developed path generator in the complex plane and the region which $\phi(s)$ $(:= s/H(s))$ maps the right-half complex plane to. Further, in order to show clearly the distinctiveness and effectiveness of the proposed technique, we derive an explicit stability condition for a

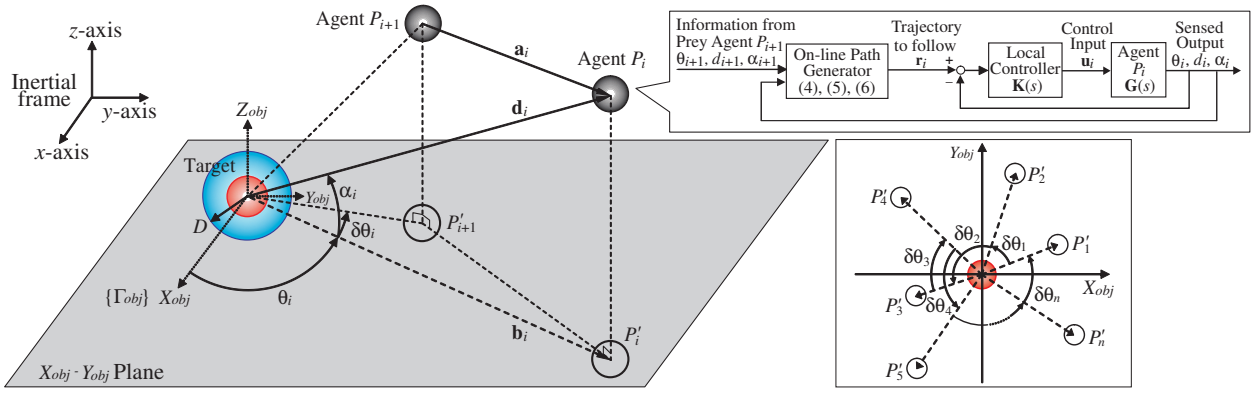

Fig. 1. Coordinate frames and notations

cyclic pursuit based path generator combined with a class of multi-agent systems; each agent is modeled as a second-order system and is locally stabilized by the proportional-integral-derivative (PID) controller. Also, optimization based approach for the design of an on-line path generator, which satisfies theoretically the derived stability condition, is presented.

2. SYSTEM DESCRIPTION AND CONTROL AIM

Consider a group of n agents dispersed in 3D space as shown in Fig. 1. All agents are ordered from 1 to n; i.e., P_1, $P_2, \cdots$, P_n. We define P_{i+1} as prey agent of P_i. Denote the position vectors of the target object and the agent P_i $(i = 1, 2, \cdots, n)$ in the inertial frame by $\mathbf{p}_o(t) \in \mathbb{R}^3$ and $\mathbf{p}_i(t) \in \mathbb{R}^3$, respectively. It is assumed that an agent P_i can measure the following vectors:

$$\mathbf{d}_i \ (:= \mathbf{p}_i - \mathbf{p}_o), \quad \mathbf{a}_i \ (:= \mathbf{p}_i - \mathbf{p}_{i+1}). \tag{1}$$

Define the target-fixed frame $\{\Gamma_{obj}\}$ where the origin is at the center of target object, and X_{obj}-, Y_{obj}- and Z_{obj}-axes are parallel to x-, y- and z-axes of the inertial frame, respectively. Let $\mathbf{b}_i$ denote the projected vector of $\mathbf{d}_i$ onto the X_{obj}-Y_{obj} plane in the target-fixed frame, and define the following scalars:

$$\theta_i = \angle(\mathbf{e}_x, \mathbf{b}_i), \quad \alpha_i = \angle(\mathbf{b}_i, \mathbf{d}_i), \quad d_i := |\mathbf{d}_i|, \tag{2}$$

where $\mathbf{e}_x$ denotes the unit vector in the X_{obj}-direction of $\{\Gamma_{obj}\}$, and $\angle(\mathbf{x}, \mathbf{y})$ denotes the counter-clockwise angle from the vector $\mathbf{x}$ to the vector $\mathbf{y}$. Then, $\mathbf{d}_i$ can be represented as $\mathbf{d}_i = [d_i \cos\theta_i \cos\alpha_i, d_i \sin\theta_i \cos\alpha_i, d_i \sin\alpha_i]^T$. Note that since $\mathbf{d}_{i+1} = \mathbf{d}_i - \mathbf{a}_i$, θ_{i+1} and $\delta\theta_i (:= \theta_{i+1} - \theta_i)$ can be calculated in a similar way based on (1). Let D denote the required distance between the target object and the agents.

Suppose that all agents P_i $(i = 1, 2, \cdots, n)$ have common system dynamics described by a MIMO plant as follows:

$$\mathbf{y}_i(s) := [\theta_i(s), d_i(s), \alpha_i(s)]^T = \mathbf{G}(s)\mathbf{u}_i(s) \tag{3}$$

where $\mathbf{y}_i(s)$ is the system output, $\mathbf{u}_i(s)$ is the control input, and $\mathbf{G}(s) := \mathrm{diag}(G_\theta(s), G_d(s), G_\alpha(s))$. Also, assume that all agents are locally stabilized by an identical diagonal feedback controller $\mathbf{K}(s) := \mathrm{diag}(K_\theta(s), K_d(s), K_\alpha(s))$ as illustrated in Fig. 1. Thus, θ-directional closed-loop transfer functions of all agents are identical and are described as $H(s) = G_\theta(s)K_\theta(s)/(1 + G_\theta(s)K_\theta(s))$. Note that, for the sake of page limitation, we mainly consider the θ-directional control scheme in this paper. For d- and α-directional control methods, refer to Hara et al. [2007b].

Now, we consider how to form a geometric pattern for the target-enclosing operation by n agents. The detailed control objectives are stated as follows:

$(A1)$ n agents enclose the target object at uniformly spaced angle and maintain this angle,
$(A2)$ Each agent approaches to the target object and finally keeps the distance D,
$(A3)$ The angle α_i which corresponds to the altitude of each agent converges to the desired one Φ,

where D and Φ are given by the designer.

In the next section, the formation control scheme which achieves the objectives $(A1)$-$(A3)$ is developed.

3. FORMATION CONTROL BASED ON A CYCLIC PURSUIT SCHEME

It is important from the practical viewpoint to achieve the desired global behavior through a relatively simple control law using only local information. As one of the feasible methods, we present a distributed cooperative control scheme motivated by a cyclic pursuit strategy for target-enclosing task [Kim and Sugie, 2007], which realizes the required geometric formation mentioned in Section 2.

3.1 Design of a distributed on-line path generator

It is assumed that n agents are randomly dispersed in 3D space at the initial time instant as depicted in Fig. 1, where $0 < |\delta\theta_i| < 2\pi$ for $i = 1, 2, \cdots, n$, and $\sum_{i=1}^{n} \delta\theta_i = 2\pi$. Then, the distributed on-line path planning scheme for the ith agent P_i is described as (see Fig. 1)

$$\dot{\theta}_i(t) = k_1 \delta\theta_i(t), \tag{4}$$

$$\dot{d}_i(t) = k_2(D - d_i(t)), \tag{5}$$

$$\dot{\alpha}_i(t) = k_3(\Phi - \alpha_i(t)), \tag{6}$$

where k_1, k_2, and k_3 (> 0) are design parameters,

$$\begin{cases} \delta\theta_i(t) := \theta_{i+1}(t) - \theta_i(t), & i = 1, 2, \cdots, n-1 \\ \delta\theta_n(t) := \theta_1(t) - \theta_n(t) + 2\pi, & i = n. \end{cases}$$

It is important to note that the gains k_1, k_2, and k_3 should satisfy some conditions to guarantee the achievement of the desired global formation $(A1)$-$(A3)$, which will be explained later in detail. Then, the reference position $\mathbf{r}_i(t) = [r_i^1(t), r_i^2(t), r_i^3(t)]^T := [\theta_i(t), d_i(t), \alpha_i(t)]^T$ for the ith agent shown in Fig. 1 is designed by (4), (5) and (6).

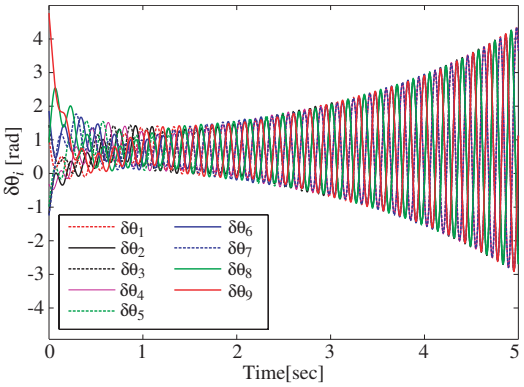

Fig. 2. Plot showing the divergence of the relative angles $\delta\theta_i(\text{rad})$ $(i = 1, 2, \cdots, 9)$

Note that, in the proposed path planning method, each agent individually decides its reference position based on the local information on only one other agent and the target object, which is probably minimum. Further, it has additional distinctive features as follows: each agent individually obtains the required information using the sensor systems implemented on its body, which means that no centralized communication mechanism between agents is introduced. Also, it is a memoryless controller in the sense that each agent determines the next behavior based only on the current position of its prey, independently of the past behavior of its prey. Thus, it is an easily implementable method from the engineering viewpoint.

Now, the control objectives $(A1)$-$(A3)$ in Section 2 can be formulated algebraically as follows:

$(A1')$ $\delta\theta_i(t) \to 2\pi/n(\text{rad})$ as $t \to \infty$,

$(A2')$ $d_i(t) \to D$ as $t \to \infty$,

$(A3')$ $\alpha_i(t) \to \Phi(\text{rad})$ as $t \to \infty$,

for $i = 1, 2, \cdots, n$. It has been proved in Kim and Sugie [2007] that path planning schemes (4)-(6) can achieve the above control objectives $(A1')$-$(A3')$ under the assumption that each agent in the group is supposed to be a point mass. However, when agent's dynamics is considered explicitly, the achievement of the stable global formation $(A1')$-$(A3')$ may not be guaranteed only by the condition that k_1, k_2 and k_3 in (4)-(6) are positive real numbers. The following example illustrates this fact clearly.

Example 1. We here only investigate the θ-directional behaviors of $n = 9$ agents for the sake of clarity. The initial values of $\theta_i(t)(\text{rad})$ are set as $\theta_1 = 0.198$, $\theta_2 = 1.269$, $\theta_3 = 0.050$, $\theta_4 = 1.491$, $\theta_5 = 1.175$, $\theta_6 = 0.189$, $\theta_7 = 2.045$, $\theta_8 = 0.793$, $\theta_9 = 1.712$. Assume that the common θ-directional agent dynamics is given by $G_\theta(s) = 1/s(s-1)$ which is stabilized by a PID controller $K_\theta(s) = 12+5/s+3s$. The reference position $r_i^1(t)$ $(= \theta_i(t))$ for agent i is designed based on (4) with $k_1 = 0.85$. The simulation is performed for $t = 5$[sec]. The time responses of $\delta\theta_i(t)$ $(i = 1, 2, \cdots, 9)$ are illustrated in Fig. 2, which clearly shows that any $\delta\theta_i$ does not converge to $2\pi/9(\text{rad})$. It demonstrates the formation instability.

One can see from the above observation that three gains k_1, k_2 and k_3 should be set carefully, in order to achieve the global formation $(A1')$-$(A3')$. Hence, in the following subsection, we will provide a simple and unified theoretical framework showing how to determine k_1, k_2 and k_3 in relation to agent's dynamics $H(s)$.

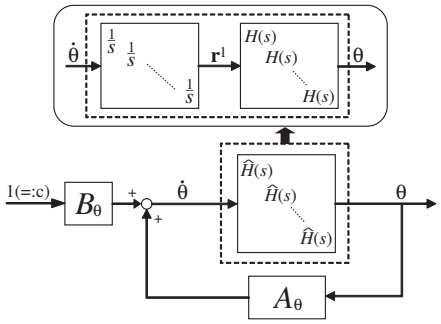

Fig. 3. Block diagram of the $\boldsymbol{\theta}$-directional formation controlled system

3.2 Formation stability analysis

In order to analyze the formation stability of multi-agent systems considered in Section 3.1, we rewrite (4) in the following vector form:

$$\begin{aligned} &\dot{\boldsymbol{\theta}}(t) = A_\theta \boldsymbol{\theta}(t) + B_\theta, \\ &A_\theta := \text{circ}(-k_1,\ k_1,\ 0,\ 0, \cdots,\ 0) \in \mathbb{R}^{n\times n}, \\ &B_\theta := [0,\ 0, \cdots,\ 0,\ 2k_1\pi]^T \in \mathbb{R}^n, \end{aligned} \tag{7}$$

where $\boldsymbol{\theta} := [\theta_1, \theta_2, \cdots, \theta_n]^T \in \mathbb{R}^n$ and 'circ' denotes the circulant matrix. Thus, the overall $\boldsymbol{\theta}$-directional control scheme can be depicted as in Fig. 3, where $\hat{H}(s) := (1/s)H(s)$ and $\mathbf{r}^1 := [r_1^1, r_2^1, \cdots, r_n^1]^T \in \mathbb{R}^n$. Here, it is assumed that $\hat{H}(s)$ is strictly proper. In the same manner, (5) and (6) can be rewritten, respectively, as

$$\dot{\boldsymbol{d}}(t) = A_d \boldsymbol{d}(t) + B_d, \tag{8}$$

$$\dot{\boldsymbol{\alpha}}(t) = A_\alpha \boldsymbol{\alpha}(t) + B_\alpha, \tag{9}$$

with $\boldsymbol{d} := [d_1, d_2, \cdots, d_n]^T \in \mathbb{R}^n$, $\boldsymbol{\alpha} := [\alpha_1, \alpha_2, \cdots, \alpha_n]^T \in \mathbb{R}^n$, $A_d := -\text{diag}(k_2, k_2, \cdots, k_2) \in \mathbb{R}^{n\times n}$, $B_d := (k_2 D)\mathbf{1}_n \in \mathbb{R}^n$, $A_\alpha := -\text{diag}(k_3, k_3, \cdots, k_3) \in \mathbb{R}^{n\times n}$, $B_\alpha := (k_3\Phi)\mathbf{1}_n \in \mathbb{R}^n$ where $\mathbf{1}_n := [1, 1, \cdots, 1]^T \in \mathbb{R}^n$. The block diagrams of the $\boldsymbol{d}$- and $\boldsymbol{\alpha}$-directional formation controlled systems have the same form with that in Fig. 3. Thus, for the sake of page limitation, we mainly consider the $\boldsymbol{\theta}$-directional control strategy.

In Fig. 3, the transfer function $\mathcal{G}_\theta(s)$ from c to $\boldsymbol{\theta}$ is obtained as

$$\mathcal{G}_\theta(s) = \left(\frac{1}{\hat{H}(s)} I_n - A_\theta\right)^{-1} B_\theta = \mathcal{F}_u\left(\begin{bmatrix} A_\theta & B_\theta \\ I_n & 0 \end{bmatrix}, \hat{H}(s) I_n\right) \tag{10}$$

where $\mathcal{F}_u$ denotes the upper linear fractional transformation (LFT). By considering the transfer function

$$L_\theta(s) = (sI_n - A_\theta)^{-1} B_\theta \tag{11}$$

which is also written as $L_\theta(s) \sim (A_\theta, B_\theta, I_n, 0)$, it follows from (10) that

$$\mathcal{G}_\theta(s) = L_\theta(\phi(s)), \quad \phi(s) := 1/\hat{H}(s). \tag{12}$$

Note that the variable 's' in (11) characterizes the frequency properties of the transfer function $L_\theta(s)$ and that $\mathcal{G}_\theta(s)$ is generated by just replacing 's' by '$\phi(s)$' in $L_\theta(s)$. Hence, we say that the transformed transfer function $\mathcal{G}_\theta(s) = L_\theta(\phi(s))$ of $L_\theta(s)$ has a generalized frequency

variable $\phi(s)$ (see Hara et al. [2007a] for details). The transfer functions $\mathcal{G}_d(s)$, $L_d(s)$, $\mathcal{G}_\alpha(s)$ and $L_\alpha(s)$ can be derived in a similar manner.

Next, in order to derive a stability condition for the system $\mathcal{G}_\theta(s)$ in (10), we first describe a key result on stability analysis of $\mathcal{G}_\theta(s)$ developed by Hara et al. [2007a]. In their paper, instead of Nyquist's graphical stability test given in Fax and Murray [2004], the domain in terms of the poles of the path generator's dynamics $L_\theta(s)$ such that $\mathcal{G}_\theta(s) = L_\theta(\phi(s))$ is stable is derived. Before we proceed, the notations are introduced: the domains Ω_+ and Ω_+^c in the complex plane are defined as

$$\Omega_+ := \phi(\mathbb{C}_+), \quad \Omega_+^c := \mathbb{C}\backslash\Omega_+. \tag{13}$$

Since $\Omega_+ = \{\lambda \in \mathbb{C} : \exists s \in \mathbb{C}_+ \text{ such that } \phi(s) = \lambda\}$, it follows that Ω_+^c can be alternatively expressed as $\Omega_+^c = \{\lambda \in \mathbb{C} : \forall s \in \mathbb{C}_+,\ \phi(s) \neq \lambda\}$. Then, the following lemma describes a sufficient condition for the existence of A_θ (A_d, A_α) so that the hierarchical system $\mathcal{G}_\theta(s)$ ($\mathcal{G}_d(s)$, $\mathcal{G}_\alpha(s)$) is stable for a given $\hat{H}(s)$.

Lemma 2. Suppose that $\hat{H}(s)$ is stable or that $\hat{H}(s)$ does not possess non-minimum phase zeros. Then, there exists A_θ (A_d, A_α) such that $\mathcal{G}_\theta(s) = L_\theta(\phi(s))$ ($\mathcal{G}_d(s) = L_d(\phi(s))$, $\mathcal{G}_\alpha(s) = L_\alpha(\phi(s))$) is stable.

Then, the key fact which describes the conditions for controllability, observability and stability of $\mathcal{G}_\theta(s)$, $\mathcal{G}_d(s)$ and $\mathcal{G}_\alpha(s)$ are provided as follows:

Proposition 3. Consider the linear systems $\mathcal{G}_\theta(s)$ in (10) and $L_\theta(s)$ in (11), and the generalized frequency variable $\phi(s)$ in (12). Assume that $\hat{H}(s)$ is strictly proper. Then, $\mathcal{G}_\theta(s)$ ($\mathcal{G}_d(s)$, $\mathcal{G}_\alpha(s)$) is controllable and observable if and only if $L_\theta(s)$ ($L_d(s)$, $L_\alpha(s)$) and $\hat{H}(s)$ are both controllable and observable. Further, $\mathcal{G}_\theta(s) = L_\theta(\phi(s))$ ($\mathcal{G}_d(s) = L_d(\phi(s))$, $\mathcal{G}_\alpha(s) = L_\alpha(\phi(s))$) is stable if and only if all the poles of $L_\theta(s)$ (L_d, L_α) belong to Ω_+^c in (13).

The proof can be found in Hara et al. [2007a]. The above proposition means that the stability of $\mathcal{G}_\theta(s)$ can be judged by just looking at the locations of eigenvalues of A_θ in relation to a domain Ω_+^c which is determined by using $\hat{H}(s)$. It is important to note from Lemma 2 and Proposition 3 that for the case where $\hat{H}(s)$ does not possess non-minimum phase zeros, there exists a domain Ω_+^c containing the origin, and the eigenvalues of A_θ (A_d and A_α) can be placed in this domain.

Finally, we present the following theorem which says that the global formation stability (i.e., $(A1')$, $(A2')$ and $(A3')$) is guaranteed as long as nonzero $n-1$ poles of $L_\theta(s)$ and all the poles of $L_d(s)$ and $L_\alpha(s)$ belong to a domain Ω_+^c.

Theorem 4. Consider the system of n agents. It is assumed that all agents are randomly dispersed in 3D space at the initial time instant as shown in Fig. 1, where $0 < |\delta\theta_i| < 2\pi$ for $i = 1, 2, \cdots, n$, and $\sum_{i=1}^n \delta\theta_i = 2\pi$. Also, suppose that (i) $n-1$ poles of $L_\theta(s)$ (except for one zero pole) belong to Ω_+^c, (ii) all the poles of $L_d(s)$ and $L_\alpha(s)$ belong to Ω_+^c; i.e., $\mathcal{G}_\theta(s)$, $\mathcal{G}_d(s)$ and $\mathcal{G}_\alpha(s)$ are stable. Then, the path planning schemes (4)-(6) achieve $(A1')$-$(A3')$ simultaneously.

This fact can be easily proved based on the result of Kim and Sugie [2007]. The above theorem implies how

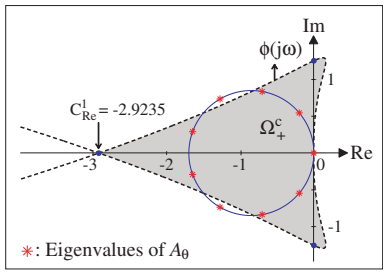

Fig. 4. The domain Ω_+^c and the eigenvalues of A_θ

to determine k_1, k_2 and k_3 of (4)-(6) in order to guarantee that all agents assemble into the desired formation around the target object in 3D space. For example, consider the multi-agent dynamical system given in Example 1, where k_1 was set as $k_1 = 0.85$. In that case, the pole locations of $L_\theta(s)$ and the domain Ω_+^c are as illustrated in Fig. 4. It verifies that two poles of $L_\theta(s)$ do not belong to Ω_+^c. Consequently, one reaches the conclusion that $(A1')$ cannot be achieved, which is evident from Fig. 2.

4. TARGET-ENCLOSING FORMATION CONTROL FOR A CLASS OF MULTI-AGENT SYSTEMS

In this section, we provide a constructive methodology that describes the domain Ω_+^c in the complex plane when the transfer function $\hat{H}(s)$ is specified. Further, we present how to design k_1, k_2 and k_3 in (4)-(6) guaranteeing that all nonzero poles of $L_\theta(s)$ and all the poles of $L_d(s)$ and $L_\alpha(s)$ belong to Ω_+^c.

4.1 Multi-agent systems stabilized by PID controllers

We take a particular rational function for $\hat{H}(s)$ to illustrate the procedure to construct Ω_+^c in the complex plane. Suppose that the generalized frequency variable $\phi(s)$ is defined as

$$\begin{aligned}\phi(s) = \frac{1}{\hat{H}(s)} &= \frac{\frac{1}{\zeta k_p t_i^2} s^4 \left(\frac{t_d}{t_i} + \frac{\xi}{\zeta k_p t_i}\right) s^3 + s^2 + s}{\frac{t_d}{t_i} s^2 + s + 1} \\ &=: \frac{bs^4 + (a+c)s^3 + s^2 + s}{as^2 + s + 1},\end{aligned} \tag{14}$$

which corresponds to the case when the θ-directional agent dynamics $G_\theta(s) = \zeta/(s(s+\xi))$, $\zeta > 0$, and the PID controller $K_\theta(s) = k_p(1 + 1/t_i s + t_d s)$ where k_p, t_i and t_d (> 0) are proportional gain, integral and derivative times, respectively (see Hara et al. [2007b] for details). Suppose that $H(s)(= s\hat{H}(s))$ is stable so that $a + c > b$. It is easily verified from (14) that $\hat{H}(s)$ has no non-minimum phase zeros.

Then, we characterize the domains Ω_+ and Ω_+^c in the complex plane. These regions are partitioned by the image of $\phi(j\omega)$ in (14) where $\omega \in \mathbb{R}$. In order to illustrate Ω_+^c clearly, we first define the real and imaginary parts of $\phi(j\omega)$ in (14), $f(\omega) := \mathrm{Re}[\phi(j\omega)]$ and $g(\omega) := \mathrm{Im}[\phi(j\omega)]$, as follows:

$$f(\omega) = \frac{\omega^4(-ab\omega^2 + b - c)}{(1 - a\omega^2)^2 + \omega^2}, \tag{15}$$

$$g(\omega) = \frac{(a^2 + ac - b)\omega^5 + (1 - 2a - c)\omega^3 + \omega}{(1 - a\omega^2)^2 + \omega^2}. \tag{16}$$

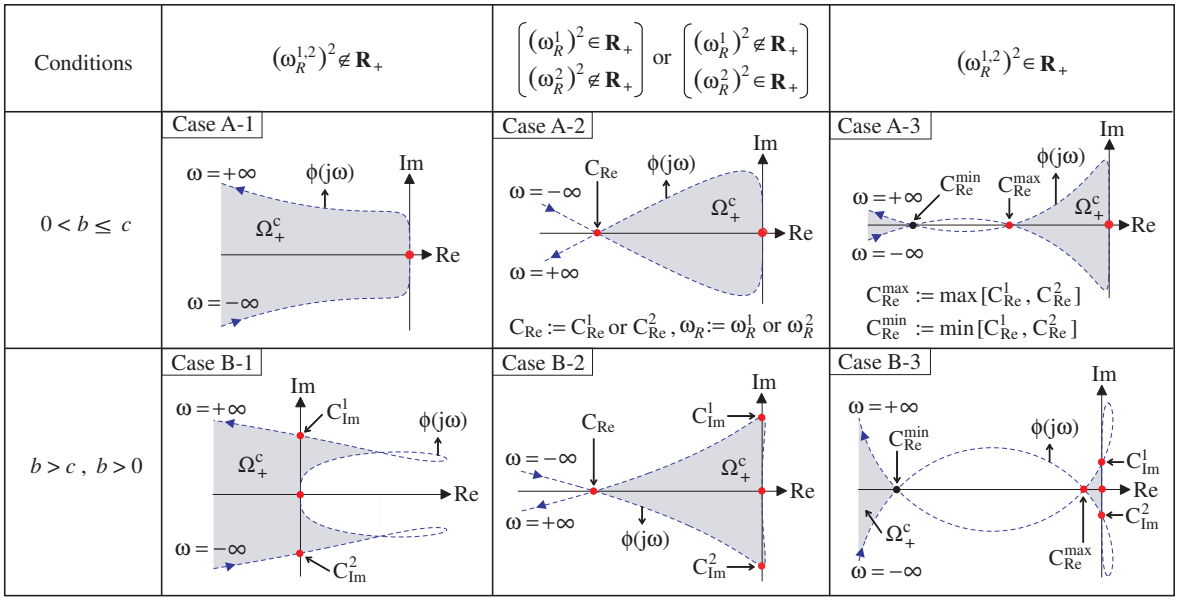

Fig. 5. The image of $\phi(j\omega)$ and the domain Ω_+^c

The intersecting points of $\phi(j\omega)$ and the imaginary axis can be easily obtained by finding ω_I which satisfies $f(\omega_I) = 0$ and then calculating $g(\omega_I)$. Similarly, the intersecting points of $\phi(j\omega)$ and the real axis can be determined from $f(\omega_R)$ where ω_R satisfies $g(\omega_R) = 0$. In this case, the image of $\phi(j\omega)$ yields six types of diagrams as illustrated in Fig. 5, where $\mathbf{R}_+$ denotes the positive real number. If $b > c$ which is equivalent to $\xi < (1/t_i)$, the image of $\phi(j\omega)$ corresponds to Case A-1, A-2 or A-3; otherwise, it corresponds to Case B-1, B-2 or B-3. In this figure, C_{Im}^1 and C_{Im}^2 are determined as $C_{Im}^{1,2} = g(\omega_I^{1,2})$, where

$$\omega_I^{1,2} = \pm\left[(b-c)/ab\right]^{1/2} \in \mathbb{R}.$$

On the other hand, C_{Re}^1 and C_{Re}^2 are determined as $C_{Re}^{1,2} = f(\omega_R^{1,2})$, where

$$(\omega_R^{1,2})^2 = \frac{(2a+c-1) \pm \left[c^2 - 2(2a-2b+c)+1\right]^{1/2}}{2(a^2+ac-b)} \in \mathbb{R}.$$

Refer to Hara et al. [2007b] for the case of PD controller $K(s) = k_p(1+t_d s)$.

In the following subsection, we present one of the methods to determine k_1, k_2 and k_3 in (4)-(6) which guarantees that all nonzero poles of $L_\theta(s)$ and all the poles of $L_d(s)$ and $L_\alpha(s)$ belong to Ω_+^c in Fig. 5.

4.2 Determination of k_1, k_2 and k_3

First, it is important to note that the eigenavlues of A_θ can be written in the following complex form, since it is a circulant matrix (see Kim and Sugie [2007]):

$$\lambda_i = k_1\left[\cos\left(\frac{2\pi(i-1)}{n}\right) - 1\right] + jk_1 \sin\left(\frac{2\pi(i-1)}{n}\right).$$

Since $k_1 > 0$, A_θ has exactly one zero eigenvalue, λ_1, while the remaining $n-1$ eigenvalues λ_i, $i = 2, 3, \cdots, n$, lie strictly in the left-half complex plane; i.e., these are located on the circumference of radius k_1 whose center is at $(-k_1, 0)$ as illustrated in Fig. 6.

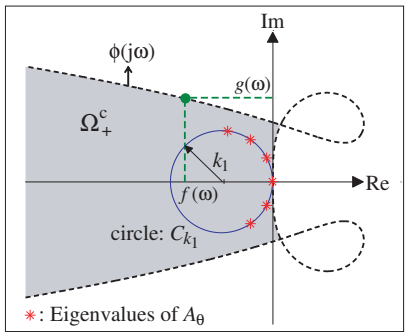

Fig. 6. The eigenvalues λ_i $(i = 1, 2, \cdots, n)$ of A_θ and the domain Ω_+^c

Therefore, all nonzero eigenvalues λ_i $(i = 1, 2, \cdots, n)$ of A_θ are placed in the domain Ω_+^c, if the design parameter k_1 satisfies the condition $(f(\omega)+k_1)^2 + g^2(\omega) \ge k_1^2$ for $\forall\omega \in \mathbb{R}$. In other words, the maximum of k_1, which guarantees that a circle C_{k_1} in Fig. 6 exists inside of Ω_+^c, can be found by solving the optimization problem:

[Constrained optimization problem]

For $f(\omega)$ in (15) and $g(\omega)$ in (16), solve

$$k_{1,\max} := \arg\max_{k_1,\omega} k_1 \tag{17}$$

subject to $k_1 > 0$ and

$$(f(\omega)+k_1)^2 + g^2(\omega) \ge k_1^2, \tag{18}$$

where the range of $\omega \in \mathbb{R}$ is set as follows: (i) $\omega > 0$ for Case A-1, (ii) $0 < \omega \le \omega_R^1$ $(\omega_R^1 > 0)$ for Cases A-2 and A-3, (iii) $\omega \ge \omega_I^1$ for Case B-1, (iv) $\omega_I^1 \le \omega \le \omega_R^1$ $(\omega_R^1 > 0)$ for Cases B-2 and B-3.

Hence, if k_1 in (4) is set as $0 < k_1 < k_{1,\max}$, then all nonzero poles of $L_\theta(s)$ belong to Ω_+^c illustrated in Fig. 5.

Finally, we consider the conditions for k_2 and k_3 in (5)-(6). Noting that the eigenvalues of A_d and A_α in (8)-(9) are, respectively, $-k_2(<0)$ and $-k_3(<0)$, the following conditions are easily derived from Fig. 5:

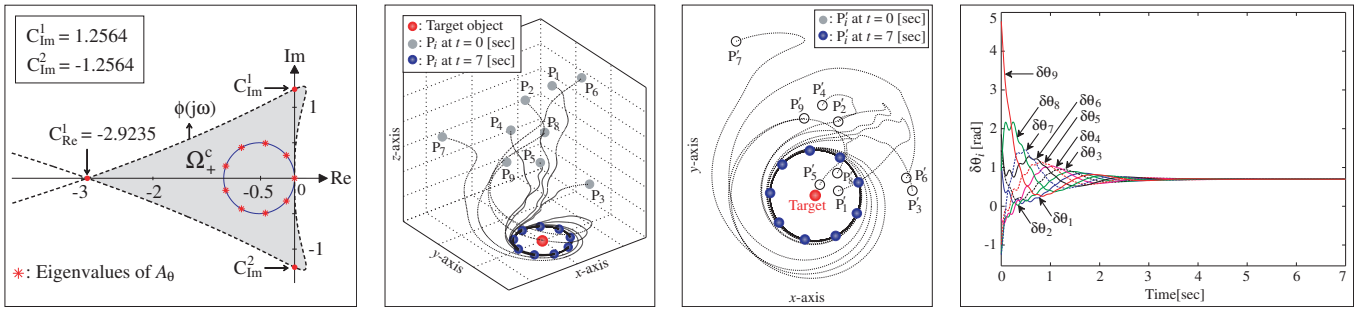

(a) Domain Ω^{c}_{+} and nine eigenvalues of A_θ ($k_1 = 0.5$)

(b) Position trajectories of all agents P_i ($i = 1, \cdots, 9$)

(c) Planar trajectories of all agents P_i ($i = 1, \cdots, 9$)

(d) Plot showing the convergence of the angles $\delta\theta_i$ ($i = 1, \cdots, 9$)

Fig. 7. Simulation results of the proposed distributed formation control scheme

(1) Cases A-1 & B-1: k_2 and k_3 can take any positive real number, since $\phi(j\omega)$ does not intersect with the real axis except at the origin.

(2) Cases A-2 & B-2: $\begin{cases} \mathrm{C}_{\mathrm{Re}} < -k_2 < 0, \\ \mathrm{C}_{\mathrm{Re}} < -k_3 < 0. \end{cases}$

(3) Cases A-3 & B-3: $\begin{cases} \mathrm{C}^{\max}_{\mathrm{Re}} < -k_2 < 0 \text{ or } -k_2 < \mathrm{C}^{\min}_{\mathrm{Re}}, \\ \mathrm{C}^{\max}_{\mathrm{Re}} < -k_3 < 0 \text{ or } -k_3 < \mathrm{C}^{\min}_{\mathrm{Re}}. \end{cases}$

4.3 Illustrative example

To illustrate the dynamic performance of the proposed distributed cooperative control scheme, a simulation is performed. Here, $n = 9$ agents are randomly dispersed in 3D space at first and finally should achieve the required formation stated in Section 2. Specifically, the desired formation is chosen to be given by $\delta\theta_i = 2\pi/9(\mathrm{rad})$ $(i = 1, 2, \cdots, 9)$, $D = 5$ and $\Phi = 0(\mathrm{rad})$. The initial values of $\alpha_i(t)(\mathrm{rad})$ and $d_i(t)$ are $\alpha_1 = \alpha_5 = 1.484$, $\alpha_2 = \alpha_6 = 1.222$, $\alpha_3 = 0.596$, $\alpha_4 = 1.047$, $\alpha_7 = 0.698$, $\alpha_8 = 1.396$, $\alpha_9 = 0.960$, $d_1 = d_6 = 30$, $d_2 = d_7 = 25$, $d_3 = 13$, $d_4 = d_8 = 20$, $d_5 = d_9 = 15$. The initial values of $\theta_i(t)$ are identical to those of Example 1. Letting $G(s) = 1/s(s-1)$ and $K(s) = 12 + 5/s + 3s$, the image of $\phi(j\omega)$ corresponds to Case B-2 in Fig. 5. Consequently, we set $0 < k_1 = 0.5 < k_{1,\max} = 0.7856$, $0 < k_2 = 0.3 < k_{2,\max} = 2.9235$ and $0 < k_3 = 0.3 < k_{3,\max} = 2.9235$. Here, $k_{1,\max}$ is obtained through the constrained particle swarm optimization method proposed by Maruta et al. [2008]. Nine eigenvalues of A_θ belong to the domain Ω^{c}_{+}, which is confirmed in Fig. 7(a). The simulation results are shown in Figs. 7(b)-7(d). First, Fig. 7(b) illustrates the resulting position trajectories of a group of nine agents during the simulation: the agents assemble into the desired configuration. Fig. 7(c) depicts the trajectories of all agents projected onto x-y plane. They show that all agents converge to a circular formation around the target object and maintain the form of an equilateral and equiangular polygon. The time responses of $\delta\theta_i$ are plotted in Fig. 7(d), where $\delta\theta_i$ finally converges to $2\pi/9(\mathrm{rad})$. It clearly demonstrates that the control goals $(A1')$-$(A3')$ mentioned in Section 3 are achieved.

5. CONCLUSION

In this paper, we proposed a design methodology of a distributed cooperative controller for target-enclosing operations by multiple dynamic agents. To this end, we first presented an on-line path generator design method based on a cyclic pursuit scheme. Then, we provided the stability condition which the developed path generator should satisfy. This condition was derived based on a considerably simple unified stability analysis method for hierarchical large-scale linear systems with a generalized frequency variable. The formation control scheme combined with a cyclic pursuit based distributed on-line path generator satisfying the derived stability condition guarantees the required global formation stability with theoretical rigor. Further, in order to show clearly its distinctive features, we addressed how to develop a cyclic pursuit based formation control strategy for a class of multi-agent systems where each agent is modeled as a second-order system and is locally stabilized by a PID controller. Its effectiveness was verified through a simulation example.

REFERENCES

J. A. Fax and R. M. Murray. Information flow and cooperative control of vehicle formations. *IEEE Trans. Autom. Contr.*, 49(9):1465–1476, 2004.

S. Hara, T. Hayakawa, and H. Sugata. Stability analysis of linear systems with generalized frequency variables and its application to formation control. In *Proc. of the 46th IEEE Conference on Decision and Control*, pages 1459–1466, New Orleans, LA, USA, 2007a.

S. Hara, T.-H. Kim, and Y. Hori. Distributed formation control for target-enclosing operation by multiple dynamic agents based on a cyclic pursuit strategy. Technical report, METR 2007-62, the University of Tokyo, 2007b. (available at http://www.keisu.t.u-tokyo.ac.jp/research/techrep/index.html).

T.-H. Kim and T. Sugie. Cooperative control for target-capturing task based on a cyclic pursuit strategy. *Automatica*, 43(8):1426–1431, 2007.

J. A. Marshall, M. E. Broucke, and B. A. Francis. Formations of vehicles in cyclic pursuit. *IEEE Transactions on Automatic Control*, 49(11):1963–1974, 2004.

I. Maruta, T.-H. Kim, and T. Sugie. Synthesis of fixed-structure H_∞ controllers via constrained particle swarm optimization. In *Proc. of the 17th IFAC World Congress*, Seoul, Korea, 2008. (to appear).

R. Olfati-Saber, J. A. Fax, and R. M. Murray. Consensus and cooperation in networked multi-agent systems. *Proceedings of the IEEE*, 95(1):215–233, 2007.